ACS APPLIED MATERIALS & INTERFACES

Research Article

www.acsami.org

Preparation of Magnetron Sputtered Thin Cerium Oxide Films with a Large Surface on Silicon Substrates Using Carbonaceous Interlayers

Martin Dubau,*[,†] Jaroslava Lavková,[†,‡] Ivan Khalakhan,[†] Stanislav Haviar,[†] Valerie Potin,[‡] Vladimír Matolín,[†] and Iva Matolínová[†]

[†]Department of Surface and Plasma Science, Faculty of Mathematics and Physics, Charles University in Prague, V Holešovičkách 2, 180 00 Prague 8, Czech Republic

[‡]Laboratoire Interdisciplinaire Carnot de Bourgogne, UMR 6303 CNRS, Université de Bourgogne, 9, Avenue Alain Savary, BP 47870, F-21078 Dijon Cedex, France

ABSTRACT: The study focuses on preparation of thin cerium oxide films with a porous structure prepared by rf magnetron sputtering on a silicon wafer substrate using amorphous carbon (a-C) and nitrogenated amorphous carbon films (CN_x) as an interlayer. We show that the structure and morphology of the deposited layers depend on the oxygen concentration in working gas used for cerium oxide deposition. Considerable erosion of the carbonaceous interlayer accompanied by the formation of highly porous carbon/cerium oxide bilayer systems is reported. Etching of the carbon interlayer with oxygen species occurring simultaneously with cerium oxide film growth is considered to be the driving force for this effect resulting in the formation of nanostructured cerium oxide films with large surface. In this regard, results of oxygen plasma treatment of a-C and CN_x films are presented. Gradual material erosion with increasing duration of plasma impact accompanied by modification of the surface roughness is reported for both types of films. The CN_x films were found to be much less resistant to oxygen etching than the a-C film.

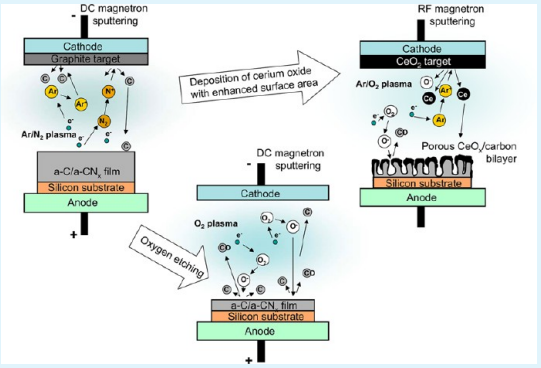

KEYWORDS: *cerium oxide thin film, magnetron sputtering, oxygen plasma, porous structure, electron microscopy, atomic force microscopy*

1. INTRODUCTION

In recent years, cerium oxide based materials such as Pt−cerium oxide have received much attention because of their excellent catalytic properties for a variety of reactions.[1−4] Among others, fuel cells offer an interesting application field of these materials. In the earlier studies[5−8] it was shown that sputtered thin Pt or Sn containing cerium oxide films, which had been deposited on the anode side of a fuel cell, exhibited a higher specific power compared to a conventional Pt−Ru catalyst. Besides the large scale fuel cells, there is also an increasing interest in miniature fuel cells fabricated on silicon,[9,10] which could be used as an on-chip power supply for portable electronic devices. However, a large active surface is generally an important requirement to improve the catalytic performance of catalysts. This leads to difficulties especially if thin film catalysts have to be realized on flat substrates such as silicon. One possibility to overcome this problem is a modification of the silicon substrate itself. Porous silicon is often used as a catalyst support, as a gas diffusion layer, or even as a membrane in micro fuel cells.[9,11] The fabrication of porous silicon is usually realized via electrochemical etching of silicon in a HF containing solution. An alternative to this method is the direct deposition of porous thin film catalysts on the flat silicon substrate. In our previous studies[7,8,12,13] we showed that magnetron sputtered cerium oxide based thin film catalysts exhibit a porous structure on carbon nanotubes and glassy carbon substrates. This effect was explained to be the result of an etching process of the carbon substrate by oxygen species (ions, radicals, ...), which occurs simultaneously with cerium oxide deposition.

Currently, a detailed study of the growth mechanism of porous thin cerium oxide films prepared by magnetron sputtering on carbon substrates revealing the influence of process parameters (e.g., deposition rate, composition of working gas, deposition time) on the structure and morphology of these films is in preparation.

In this study, we present the possibility of preparing cerium oxide thin films (thickness equal to or less than 30 nm) with a large surface on silicon substrates using carbon materials that are sputtered films of amorphous carbon (a-C) and nitrogenated amorphous carbon (CN_x), as an interlayer. We demonstrate that the surface morphology and the microstructure of the prepared bilayers are strongly affected by the cerium oxide film preparation conditions. In particular, the key

Received: November 5, 2013
Accepted: December 27, 2013
Published: December 27, 2013

   dx.doi.org/10.1021/am4049546 | *ACS Appl. Mater. Interfaces* 2014, 6, 1213−1218

role of oxygen amount in the working gas used for the cerium oxide film deposition is pointed out.

The first part of this study focuses on the investigation of the behavior of a-C and CN_x films in oxygen plasma including the comparison of the degree of material erosion and changes of the surface morphology. These results are correlated with the microstructural differences of cerium oxide films depending on the used carbon interlayer. The second part deals with the deposition of cerium oxide films on silicon supported a-C and CN_x interlayers. Investigations related to the surface morphology as well as the structure of the resulting bilayers have been performed. The third part covers the influence of the concentration of oxygen in the process gas used for the sputter deposition of cerium oxide films on the morphology of the carbon/cerium oxide bilayers prepared on silicon substrates.

2. EXPERIMENTAL DETAILS

Silicon wafers of (100) orientation were used as substrates. The a-C and the CN_x films were prepared by dc magnetron sputtering from a 2 in. diameter graphite target (Goodfellow, purity of 99.997%) using a commercial modular high vacuum coating system MED020 (BALTEC). Details of the deposition process can be found in Table 1.

Table 1. Summary of the Deposition Parameters for a-C and CN_x Films

parameter	a-C	CN_x
target−substrate distance	50	50
target material	pure graphite	pure graphite
working gas	pure Ar	pure N_2
gas pressure, Pa	0.8	4
discharge current	20	20 mA
discharge voltage, V	∼540	∼560
deposition rate, nm/min	3.7 ± 0.4	30 ± 3

The oxygen plasma treatment was carried out in the MED020 system as well, using an etching device consisting of a ring-shaped driven Al electrode placed 2 cm above the grounded substrate holder. Accordingly, the dc discharge was ignited between the electrode and the substrate holder. The process gas was pure oxygen at a total pressure of 20 Pa. The discharge current was set equal to 1.7 mA, and the discharge voltage automatically adjusted by the MED020 system was ∼430 V.

The deposition of cerium oxide thin films has been carried out using the rf magnetron sputtering technique in a magnetron sputtering system of our own construction with a residual gas pressure of less than 4×10^{-4} Pa. A CeO_2 disk (Kurt Lesker, 2 in. diameter, purity of 99.99%) placed 90 mm below the substrate holder (grounded) has been used as a target. The working gas was either pure argon at a pressure of 0.4 Pa or an argon/oxygen gas mixture kept at the same total pressure. The oxygen partial pressure was adjusted with a needle valve and measured using a vacuum gauge. The input discharge power was 24 or 15 W, respectively. The corresponding deposition rates were approximately 0.4 and 0.12 nm/min.

Morphology and structure of the prepared samples have been characterized by means of scanning electron microscopy (SEM), transmission electron microscopy (TEM), and atomic force microscopy (AFM). A Tescan MIRA 3 SEM has been operated with electron beam energy of 30 keV. The TEM observations were carried out using a JEOL 2100 (LaB_6) electron microscope with electron beam energy of 200 keV. The samples for TEM observations in a form of thin lamellas have been prepared from the thin film samples by means of a "lift-out" technique[14] using a dual beam microscope LYRA (SEM-FIB, Tescan) equipped with a gas injection system (GIS). A platinum or silicon oxide protection layer that simultaneously delivers sufficient material contrast in TEM was deposited on the surface of each sample. The lamellas were picked up with a tungsten standard probe tip (Omniprobe) and placed on copper TEM grids (Omniprobe). The thickness of each lamella was reduced to approximately 60 nm via a two-step polishing technique using gallium ions at an energy of 30 keV at first. Subsequently the ion energy has been reduced to 10 keV in order to minimize the amorphous contamination layer formed on the sample during the first polishing step.

The AFM was operated in the semicontact mode using a FESP tip (Bruker) with a nominal tip radius of 8 nm. All AFM images have been measured with the same type of tip in order to ensure the comparability of the determined values of surface roughness (R_a). The R_a values have been calculated using Nanoscope software from 1 μm × 1 μm AFM images.

The thickness of all deposited films has been measured ex situ by two methods. The first is using step height measurements with an atomic force microscope (Veeco di MultiMode V). For this purpose, one part of a silicon substrate was masked with a drop of varnish, which was removed after the deposition or etching process. The resulting step was used for the film thickness measurement. Second, the thickness of the deposited films was determined from TEM micrographs of sample cross sections. The corresponding uncertainty of the film thickness is about ±10% in both cases and is given mainly by an inhomogeneity in the sputtering process during the carbon or cerium oxide deposition.

3. RESULTS AND DISCUSSION

3.1. Oxygen Plasma Treatment of a-C and CN_x Films on Silicon Substrates. Several samples of as-prepared a-C and CN_x films supported by silicon substrate have been simultaneously treated in oxygen plasma for different time periods (10, 20, 30, and 40 min). The thicknesses and roughnesses of the carbonaceous films were compared afterward. The SEM plan-view micrographs together with the TEM cross-section images and the corresponding AFM images of the carbon layers before and after oxygen plasma etching for two selected treatment periods (30 and 40 min) are shown in

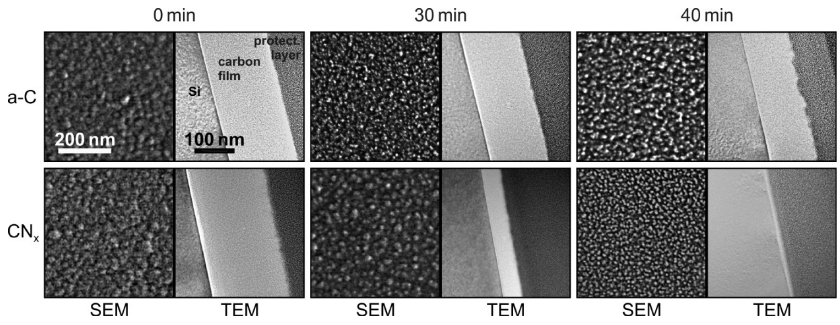

Figure 1. SEM plan-view micrographs and TEM cross-section images of the a-C and CN_x films on silicon wafer prior to and after oxygen plasma treatment as a function of etching time.

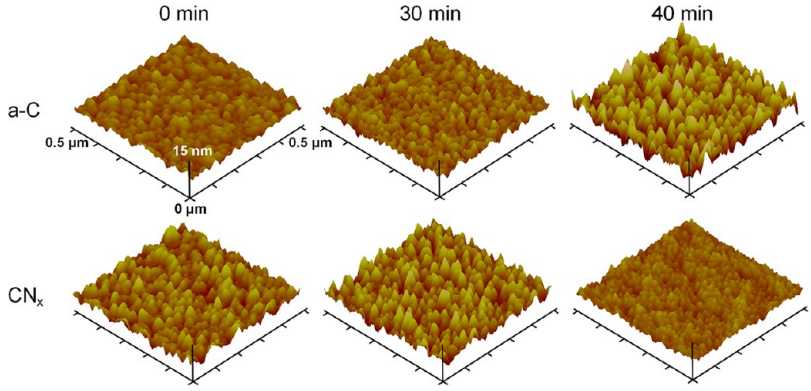

Figure 2. AFM micrographs of a-C prior and after oxygen plasma treatment as a function of etching time.

Figures 1 and 2. In Figure 3 the results of film thickness measurements and the calculated values of surface roughness R_a

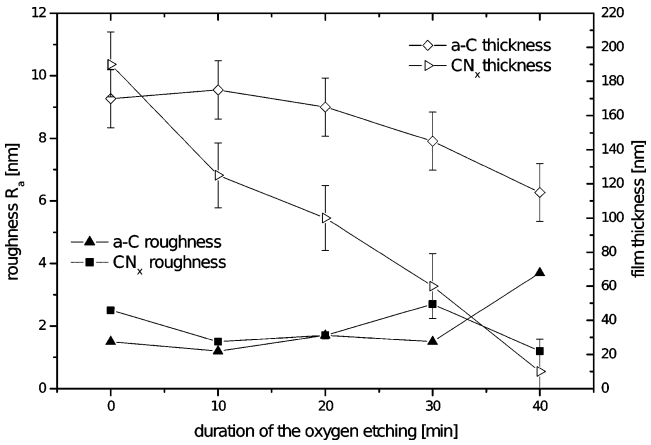

Figure 3. Dependence of the carbon films thickness and roughness on oxygen plasma etching time.

based on the TEM and AFM observations, respectively, are presented for both types of carbon films prior to and after the oxygen plasma treatment. Both as-prepared films are compact without any visible structure in the TEM cross-section view exhibiting a rather flat surface with slightly corrugated structure with shallow dips. Significant material erosion can be observed for both carbonaceous films during oxygen plasma etching as a gradual fading of the deposited layers accompanied by formation of a fine grainy surface. In the case of the a-C film the oxygen plasma treatment for 40 min leads to a deepening of the dips, which is visible in the TEM micrograph (Figure 1) as well as in the AFM image (Figure 2), resulting in higher R_a value.

In contrast, the surface morphology of the CN_x film looks nearly unchanged after 30 min of plasma treatment. Likewise, the R_a value is comparable with the as-prepared CN_x film in spite of the large amount of material etched away. However, a slight decrease in surface roughness of the deposited CN_x layer can be observed after 10 and 20 min of oxygen plasma treatment (not shown herein) followed by its increase after 30 min of the plasma etching. After 40 min of plasma treatment a considerable flattening of the CN_x surface accompanied by the formation of very fine grainy structure can be observed. These effects are connected to a nearly complete removal of the CN_x film visible in the TEM image.

The measurements of the thicknesses of the carbonaceous films as a function of the etching time (see Figure 3) lead to the conclusion that the CN_x film is significantly less resistant to oxygen plasma than the a-C film.

3.2. Sputter Deposition of Cerium Oxide Layers on the a-C and CN_x Films in Pure Argon. In order to study the growth of cerium oxide on the carbonaceous films, thin layers of cerium oxide about 5, 20, and 30 nm thick were deposited on the silicon supported a-C and CN_x films. In order to suppress carbon erosion caused by oxygen during magnetron sputtering,

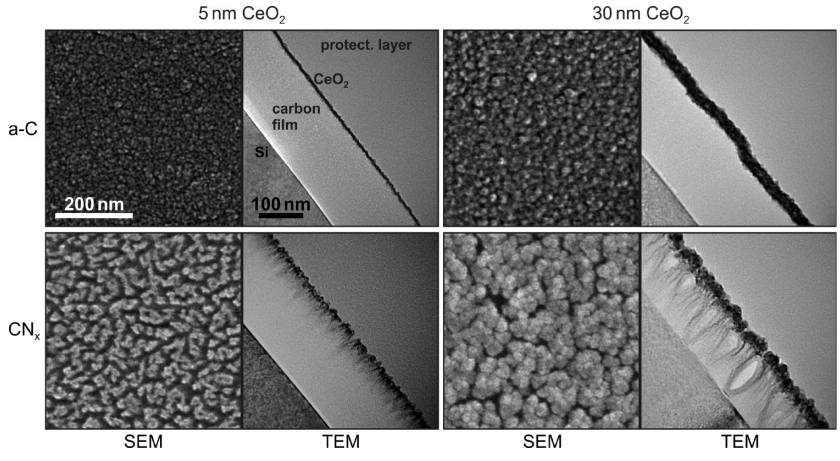

Figure 4. SEM plan-view micrographs and TEM cross-view images of cerium oxide of two different thicknesses deposited on the carbon films.

dx.doi.org/10.1021/am4049546 | ACS Appl. Mater. Interfaces 2014, 6, 1213−1218

the cerium oxide film deposition was performed in pure argon. Accordingly, oxygen species causing etching of the carbon interlayer might originate only from the cerium oxide target or the residual gas (mainly consisting of water vapor). The cerium oxide film thickness was determined after the deposition via step height measurements. The SEM and TEM micrographs of prepared cerium oxide films on both materials are presented in Figure 4. The a-C supported cerium oxide films exhibit a grainy surface structure for all investigated film thicknesses. The corresponding TEM images of the cross section of each sample show that the a-C/cerium oxide bilayers have a compact structure comparable to the one observed in the case of cerium oxide deposited directly on the silicon surface.[6,15] In accordance with the SEM images, the surface of these a-C supported cerium oxide films is nearly flat. In contrast, the cerium oxide films deposited on the silicon supported CN_x interlayers exhibit more and more porous surface structure as the cerium oxide film grows. The resulting CN_x/cerium oxide bilayers are discontinuous with a pillar structure. The pillars with cerium oxide on the top are separated by holes, the depth of which increases with increasing thickness of the cerium oxide film because the longer is the time of the cerium oxide deposition, the longer is the time of the carbon etching by the plasma.

The evolution of the carbon support thickness with increasing cerium oxide layer thickness has been determined from the TEM images and can be seen in Table 2. It is shown that the thickness of the CN_x support decreases dramatically with an increasing amount of deposited cerium oxide. The observed behavior matches the behavior of CN_x layers treated in oxygen plasma as described above. It is very likely that this effect together with the formation of the pillar structure can be assigned to etching of the carbon support by oxygen species contained in plasma during the cerium oxide deposition. Oxygen species interacting with the carbon support and thus removing carbon from the sample can originate from the cerium oxide target as well as from the residual gas. More details will be given below.

Table 2. Thicknesses of the Carbon Film Prior and after Cerium Oxide Deposition Determined from the TEM Images with Uncertainty of about ±10%

	thickness of the carbon interlayer [nm]	
thickness of the cerium oxide cover [nm]	a-C	CN_x
0	170	190
5	160	163
20	167	130
30	168	109

The compact structure of the a-C/cerium oxide bilayers indicates that no significant etching of the a-C support occurs during the cerium oxide film deposition at the given conditions. Furthermore, the a-C film thickness is not measurably affected by the duration of the cerium oxide film deposition in the range of uncertainty. It is expected that only at the first stage of the film formation a slight a-C film etching with oxygen takes place in the meantime until the carbon surface is not completely covered with cerium oxide. This observation is in agreement with the result of the previous section that the a-C film exhibits a significantly higher resistance against oxygen plasma than the CN_x film.

3.3. Sputter Deposition of Cerium Oxide Layers in Argon/Oxygen Gas Mixtures. In order to achieve a more intense etching of the carbon support during the cerium oxide film deposition, a small amount of oxygen has been added to the process gas. The discharge power has been reduced to P = 15 W in order to reduce the deposition rate and, as a consequence, to support the etching process of the carbon films. The thickness of the deposited oxide layers was approximately 10 nm. Figure 5 shows the SEM micrographs of cerium oxide deposited in two different argon/oxygen gas mixtures with an oxygen partial pressure of 0.001 and 0.01 Pa, respectively. Additionally, the corresponding images of a cerium oxide film deposited in pure argon at the reduced discharge power are given for comparison. It can be seen that the cerium oxide films deposited in pure argon exhibit a similar morphology, as it was observed for the higher discharge

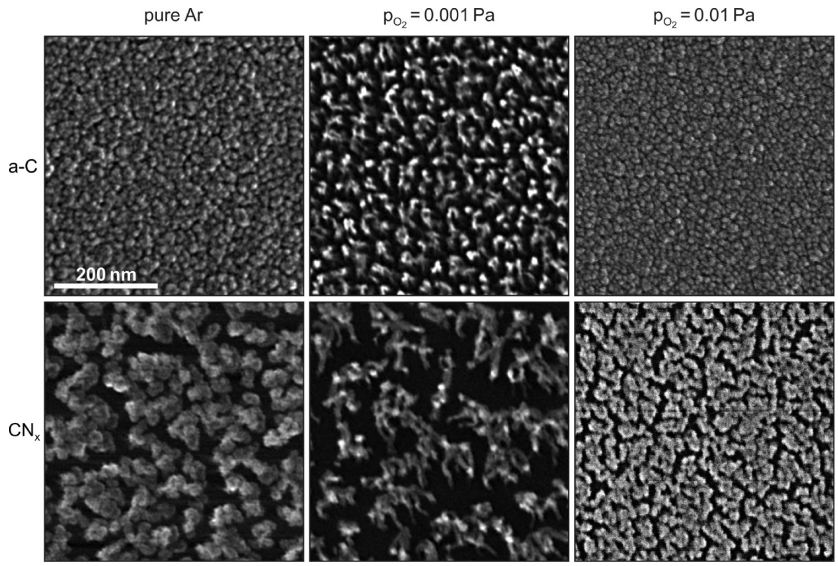

Figure 5. SEM plan-view micrographs of 10 nm cerium oxide films deposited on the carbon films in pure argon and two different argon−oxygen gas mixtures with an oxygen partial pressure of 0.001 and 0.01 Pa at total pressure of 0.4 Pa.

power presented in Figure 4. A compact cerium oxide film with a fine grainy surface structure grows on the a-C support, whereas the CN_x support enables the formation of a highly porous cerium oxide film.

The addition of 0.001 Pa of oxygen to the working gas leads to a dramatic change of the cerium oxide film morphology on both support materials due to more intensive etching of the carbon films. Consequently, the formation of well separated small wormlike islands can be observed. On the CN_x support larger and more extended islands separated by valleys are visible compared to the a-C/cerium oxide bilayer. Further increase of the partial pressure of oxygen in the working gas (0.01 Pa) does not create more open structures, contrary to what might be expected. Instead, the formation of more compact film of smoother structure in comparison with the one obtained for the deposition in pure argon can be observed. On the CN_x support, a wormlike structure of the double film is still visible. These observations indicate that the erosion of carbon at elevated partial pressure of oxygen is no longer the dominant phenomenon during cerium oxide film growth.

These results clearly show that oxygen plays a crucial role in the formation of porous cerium oxide films on carbonaceous materials. Growth mechanism of the porous layers can be thought of as the growth of a thin film of cerium oxide accompanied by simultaneous etching of the carbon interlayer on the silicon substrate. Lack of oxygen in the process gas leads to the growth of compact cerium oxide films due to an insufficient etching of the carbon support. However, the same is valid if the oxygen partial pressure is too high. In this case the formation of porous cerium oxide films is likewise prevented. This can be explained with a suppressed etching of the carbon support due to formation of a large number of nucleation centers of cerium oxide growing subsequently to small cerium oxide particles on the carbon film, which act as a barrier or an etching mask and thus reduce the availability of the carbon surface.

According to the literature,[16−19] carbon substrate modification by oxygen interaction with carbon substrate and its removal due to the formation of volatile carbon oxides (CO and CO_2) can be considered as an universal effect. Carbon erosion is one of many phenomena and parameters that are involved in the growth mechanism of cerium oxide based thin films on carbon substrates as it is shown here, which makes it possible to tune the morphology of deposited film.

The obtained results offer a possibility of preparing cerium oxide films with a large surface on silicon substrates via the use of the magnetron sputtering technique only. This is a remarkable step forward regarding the realization of micro fuel cells integrated on silicon chips using novel cerium oxide based thin film catalysts. The positive experience with platinum doped cerium oxide films with respect to the specific power determined in the case of a large scale fuel cell described in our previous work[5−8] can be transformed to the microscale using the preparation procedure described in this work. Investigations in this direction are in progress.

4. SUMMARY AND CONCLUSIONS

This work was focused on the preparation of thin sputtered cerium oxide films with a large surface area on conventional silicon substrates using sputtered amorphous carbon (a-C) and nitrogenated amorphous carbon films (CN_x) as a support interlayer. We showed that it is possible to prepare cerium oxide films with a porous structure on both supports if an appropriate argon/oxygen gas mixture is used as the process gas for the cerium oxide film deposition. The porous growth can be explained by a chemical etching of the carbon support with oxygen species which occurs simultaneously with cerium oxide film growth. In contrast, the deposition of cerium oxide in pure argon delivers compact films on the a-C support because of a lack of oxygen. However, if a CN_x film is used as a support, porous cerium oxide films grow even in pure argon. Obviously, oxygen originating from the residual gas or from the cerium oxide target is sufficient in order to achieve a considerable etching of the CN_x support during cerium oxide film growth due to its significantly lower resistance against oxygen plasma compared with the a-C film.

AUTHOR INFORMATION

Corresponding Author

*E-mail: martin.dubau@gmail.com.

Notes

The authors declare no competing financial interest.

ACKNOWLEDGMENTS

The research support was provided by The Grant Agency of Charles University under Project No. 617412, Czech Science Foundation under Grant No. 13-10396S, Agence Nationale de la Recherche within IMAGINOXE project (Grant ANR-11-JS10-001), and EU FP-7-NMP-2012 project chipCAT under Contract No. 310191. M.D. acknowledges the support of Vakuum Praha under Grant for 2013, and J.L. acknowledges the support of Conseil Régional de Bourgogne (PARI ONOV 2012). In addition, M.D. thanks Dr. Daniel Mazur, Ph.D., for careful reading of the manuscript.

REFERENCES

(1) *Catalysis by Ceria and Related Materials*, 1st ed.; Trovarelli, A., Ed.; Catalytic Science Series, Vol. 2; Imperial College Press: London, 2002.

(2) Idriss, H.; Scott, M.; Llorca, J.; Chan, S. C.; Chiu, W.; Sheng, P.-Y.; Yee, A.; Blackford, M. A.; Pas, S. J.; Hill, A. J.; Alamgir, F. M.; Rettew, R.; Petersburg, C.; Senanayake, S.; Barteau, M. A. *ChemSusChem* **2008**, *1*, 905−910.

(3) Sheng, P. Y.; Chiu, W. W.; Yee, A.; Morrison, S. J.; Idriss, H. *Catal. Today* **2007**, *129*, 313−321.

(4) Suchorski, Y.; Wrobel, R.; Becker, S.; Strzelczyk, B.; Drachsel, W.; Weiss, H. *Surf. Sci.* **2007**, *601*, 4843−4848.

(5) Václavů, M.; Matolínová, I.; Mysliveček, J.; Fiala, R.; Matolín, V. *J. Electrochem. Soc.* **2009**, *156*, B938−B942.

(6) Matolín, V.; Cabala, M.; Matolínová, I.; Škoda, M.; Václavů, M.; Prince, K. C.; Skála, T.; Mori, T.; Yoshikawa, H.; Yamashita, Y.; Ueda, S.; Kobayashi, K. *Fuel Cells* **2010**, *10*, 139−144.

(7) Fiala, R.; Khalakhan, I.; Matolínová, I.; Václavů, M.; Vorokhta, M.; Sofer, Z.; Huber, S.; Potin, V.; Matolín, V. *J. Nanosci. Nanotechnol.* **2011**, *11*, 5062−5067.

(8) Matolín, V.; Matolínová, I.; Václavů, M.; Khalakhan, I.; Vorokhta, M.; Fiala, R.; Piš, I.; Sofer, Z.; Poltierová-Vejpravová, J.; Mori, T.; Potin, V.; Yoshikawa, H.; Ueda, S.; Kobayashi, K. *Langmuir* **2010**, *26*, 12824−12831.

(9) Min, K.-B.; Tanaka, S.; Esashi, M. *J. Micromech. Microeng.* **2006**, *16*, 505−511.

(10) Lu, G. Q.; Wang, C. Y.; Yen, T. J.; Yhang, X. *Electrochim. Acta* **2004**, *49*, 821−828.

(11) Pichonat, T.; Gauthier-Manuel, B. *J. Micromech. Microeng.* **2005**, *15*, S179−S184.

(12) Matolínová, I.; Fiala, R.; Khalakhan, I.; Vorokhta, M.; Sofer, Z.; Yoshikawa, H.; Kobayashi, K.; Matolín, V. *Appl. Surf. Sci.* **2012**, *258*, 2161−2164.

(13) Khalakhan, I.; Dubau, M.; Haviar, S.; Lavková, J.; Matolínová, I.; Potin, V.; Vorokhta, M.; Matolín, V. *Ceram. Int.* **2013**, *39*, 3765−3769.
(14) Wirth, R. *Chem. Geol.* **2009**, *126*, 217−229.
(15) Bruyère, S.; Cacucci, A.; Potin, V.; Matolínová, I.; Vorokhta, M.; Matolín, V. *Surf. Coat. Technol.* **2013**, *227*, 15−18.
(16) Liu, X.; Cheng, L.; Zhang, L.; Yin, X.; Dong, N.; Zhao, D.; Hong, Z. *Int. J. Appl. Ceram. Technol.* **2013**, *10*, 168−174.
(17) Philipps, V.; Sergienko, G.; Lyssoivan, A.; Esser, H. G.; Freisinger, M.; Kreter, A.; Samm, U. *J. Nucl. Mater.* **2007**, *363*, 929−932.
(18) Belmonte, T.; Pintassilgo, C. D.; Czerwiec, T.; Henrion, G.; Hody, V.; Thiebaut, J. M.; Loureiro, J. *Surf. Coat. Technol.* **2005**, *200*, 26−30.
(19) Baker, M. A. *Thin Solid Films* **1980**, *69*, 359−368.